NG Civil Engineering
ISSN (online): 3107-569X
Volume 2, Issue 2 (April-June), 2026, 52-63

Research Article *Open Access*

GIS and AHP-Based Landslide Susceptibility Mapping of the Teesta River Basin, Eastern Darjeeling-Kalimpong Himalaya, India

Kankona Maity, Sangita Hazra*

Department of Geospatial Science, Techno India University, West Bengal, India

*Corresponding author email ID: sangitahazra2001@gmail.com

HIGHLIGHTS

- GIS, RS and AHP were integrated to map landslide susceptibility in the Teesta River Basin.
- Seventeen conditioning factors were used to classify the basin into five susceptibility zones.
- Moderate and high susceptibility zones dominated, especially in Kalimpong and Kalimpong-I sectors.

ARTICLE INFO

Article History:
Received: 10 March 2026
Revised: 21 April 2026
Accepted: 25 may 2026
Online Published: 30 June 2026

Keywords:
Landslide
Analytic Hierarchy Process (AHP)
Hazard Mapping
Geographic Information System (GIS)
Teesta River Basin

ABSTRACT

Landslides are frequent hydro-geomorphic hazards in the Eastern Himalaya due to steep slopes, weak lithology, intense monsoonal rainfall, drainage dissection and anthropogenic pressure. This study prepared a landslide susceptibility map for part of the Teesta River Basin covering Darjeeling and Kalimpong districts, West Bengal, India, using GIS, remote sensing and the Analytic Hierarchy Process. Seventeen conditioning factors, including terrain, lithology, rainfall, drainage, land use/land cover, vegetation and hydrological indices, were derived from DEM, satellite, geological, soil, rainfall and ancillary spatial datasets and integrated through weighted overlay analysis. The susceptibility map classified the area into very low, low, moderate, high and very high zones. Moderate susceptibility covered the largest area, followed by high, low, very high and very low zones. The northern and central mountainous sectors, particularly around Kalimpong and Kalimpong-I, showed higher susceptibility than the southern foothills. The map can support land-use planning, infrastructure development, disaster risk reduction and sustainable watershed management in the Teesta Himalayan landscape.

1. INTRODUCTION

Landslides are major geomorphic hazards in mountainous regions and frequently cause loss of life, damage to road networks, disruption of settlements, degradation of agricultural land and long-term environmental disturbance. Their occurrence is normally controlled by the interactions among geological, geomorphological, hydrological, climatic, and anthropogenic factors. In the Himalaya, these interactions are particularly intense because the terrain is young, tectonically active, structurally weak, highly dissected and exposed to concentrated monsoonal rainfall. Rapid road expansion, settlement growth, deforestation, tourism development and slope cutting further intensify landslide hazard in many vulnerable hill environments (Guzzetti et al., 2012; Reichenbach et al., 2018).

https://doi.org/10.66132/ngce20260205

The Darjeeling-Kalimpong sector of the Eastern Himalaya is one of the landslide-prone hill environments of India. The region is characterized by steep slopes, deeply incised valleys, variable lithological units, high drainage density and high seasonal rainfall. The Teesta River and its tributaries play an important role in valley incision, bank erosion and undercutting of slopes. In such a setting, landslide susceptibility mapping is essential for prioritizing slope-stabilization measures, regulating land-use decisions, supporting road and infrastructure planning and improving local disaster preparedness (Pradhan & Lee, 2010; Sarkar et al., 2013).

Landslide Susceptibility Mapping (LSM) identifies areas with different relative likelihoods of landslide occurrence by relating known or inferred landslide processes to conditioning variables. It does not predict the exact timing of slope failure; rather, it provides a spatial probability or relative susceptibility surface that can guide planning. With the expansion of Remote Sensing and GIS, it has become possible to compile, standardize and integrate large spatial datasets such as digital elevation models, rainfall surfaces, lithology, lineaments, drainage networks, vegetation indices and land-use/land-cover layers (Fell et al., 2008; Guzzetti et al., 2005; Van Westen et al., 2008).

Several modelling approaches are used for LSM, including heuristic, statistical, probabilistic, bivariate, multivariate and machine-learning techniques. Frequency Ratio, Weight of Evidence, Logistic Regression and Evidential Belief Function models are widely used because they quantify the spatial association between landslide occurrence and conditioning factors (Ayalew & Yamagishi, 2005; Bonham-Carter, 1994; Lee & Pradhan, 2007). Multi-Criteria Decision-Making methods, particularly the Analytic Hierarchy Process (AHP), remain useful where complete field inventories or geotechnical observations are limited. AHP allows expert knowledge and literature-supported judgment to be converted into normalized factor weights through pairwise comparison (Kayastha et al., 2013; Saaty, 1980). Recent landslide susceptibility studies in the Darjeeling-Sikkim Himalaya show that GIS-based statistical, probabilistic and decision-support models can provide reliable spatial prediction of landslide-prone areas. Kundu and Ghosh (2025) assessed landslide susceptibility in the upper Teesta River Basin using Logistic Regression, Frequency Ratio and AHP models with fifteen conditioning factors. Their validation using ROC-AUC showed very high performance for Logistic Regression and Frequency Ratio, while AHP produced a usable expert-weighted susceptibility framework.

Mandal, Biswas, and Mandal (2026) applied seven bivariate statistical models in the Lish River Basin of the Darjeeling Himalaya using 188 landslides, twenty-one causative factors and exposure information for settlements and roads. The Modified Information Value model performed best and helped identify settlements and road sections located within high-susceptibility zones. Mandal, Mondal, and Mandal (2023) used a Weight of Evidence model for Darjeeling Himalaya and validated the susceptibility output using 2,079 landslide locations, demonstrating the practical value of probabilistic modelling in the region.

Bivariate and hybrid methods have also been applied outside the Himalaya. Bachri et al. (2025) used Weight of Evidence and Frequency Ratio models in East Java, Indonesia, and reported that slope, lithology and rainfall were important controls. Poddar and Roy (2024) compared GIS-based data-driven bivariate models in the Teesta Basin and highlighted the relevance of remote sensing and geospatial modelling for highly landslide-affected Himalayan terrain. In Wayanad, Western Ghats, Pitchaimani et al. (2026) demonstrated that an AHP-GIS approach can be extended from susceptibility assessment to vulnerability assessment of buildings, roads and agricultural land.

These studies collectively indicate that slope instability in mountainous environments is rarely controlled by a single factor. Robust susceptibility mapping therefore requires an integrated spatial framework that combines terrain, geology, drainage, rainfall, land cover and vegetation information. The present study follows this integrated approach but focuses specifically on AHP-based weighted overlay mapping for the Teesta River Basin.

The present study employs Geographic Information System (GIS), Remote Sensing (RS) and the Analytic Hierarchy Process (AHP) to develop a landslide susceptibility map for a selected part of the Teesta River Basin in the Eastern Darjeeling–Kalimpong Himalaya. The study integrates seventeen landslide-conditioning factors representing topographic, geological, hydrological, climatic, environmental and land-use/land-cover influences on slope instability. The main objectives are to prepare a GIS-based spatial database of these conditioning factors, assign their relative weights through the AHP method, examine the consistency of the pairwise comparison matrix, and generate a landslide susceptibility map by classifying the study area into very low, low, moderate, high and very high susceptibility zones. The resulting map is expected to support the identification of landslide-prone areas and provide useful inputs for disaster risk reduction, land-use planning, infrastructure development and environmental management in this fragile Himalayan basin.

2. MATERIALS AND METHODS

2.1 Study area

The study area forms part of the Teesta River Basin in the Eastern Himalaya and lies within Darjeeling and Kalimpong districts of West Bengal, India. It extends approximately from 26°52′N to 27°09′N latitude and 88°24′E to 88°35′E longitude (Figure 1) . The terrain is hilly and highly dissected, with steep valley sides, a dense drainage network and the Teesta River as the main fluvial system. Heavy monsoonal rainfall, structurally weak and weathered geological units, active erosion and human activities such as road construction, settlement expansion and agriculture make the basin highly vulnerable to landslides. The area is therefore suitable for GIS-based landslide susceptibility analysis.

2.2 Data collection and software used

The analysis used DEM-derived terrain and hydrological layers, satellite-derived vegetation and land-cover information, geological and soil layers, rainfall information and a landslide inventory layer. All layers were projected, rasterized where necessary, reclassified and resampled to a common spatial resolution before overlay analysis. The key software and spatial datasets used in the study are summarized in Tables 1 and 2.

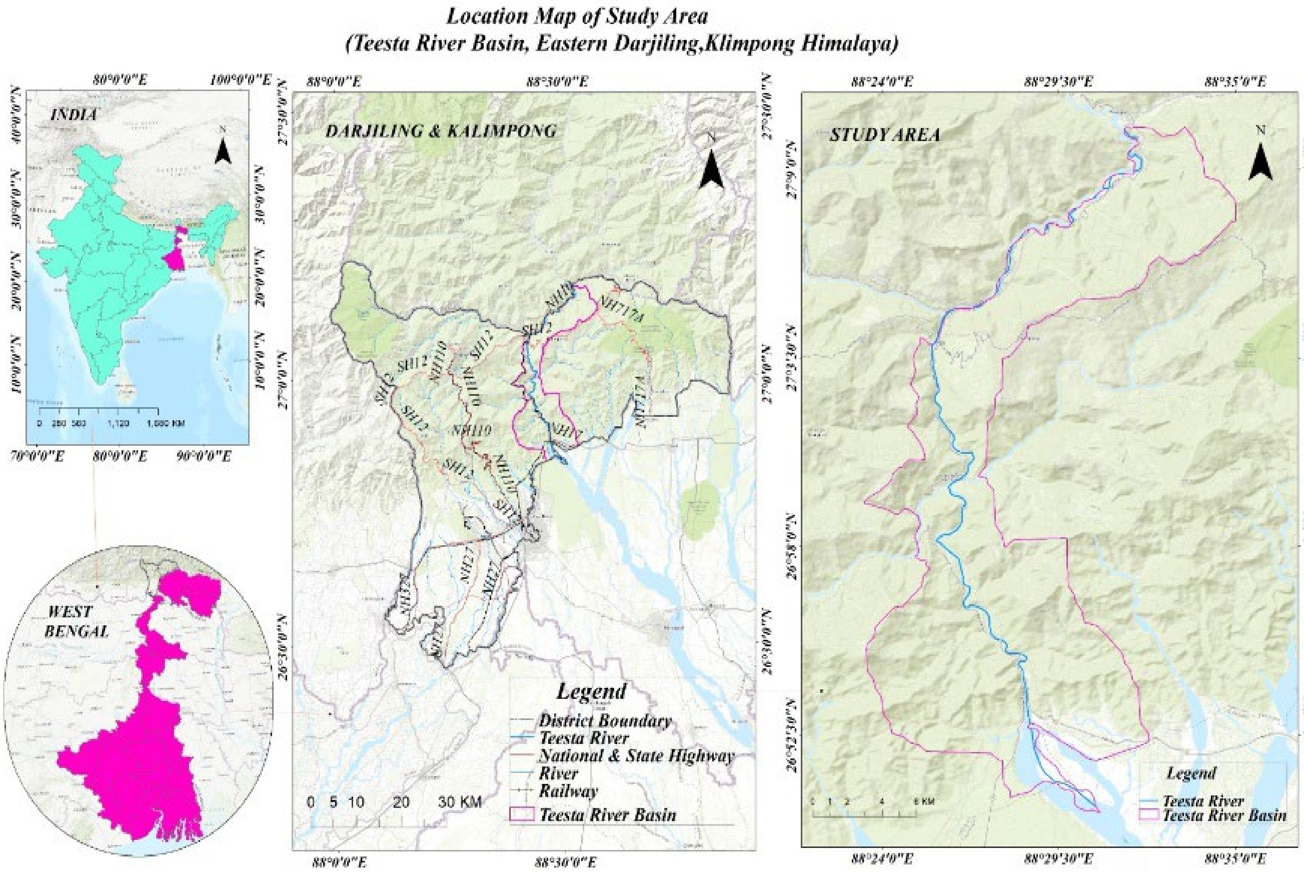

Figure 1. Location map of the study area in the Teesta River Basin, Eastern Darjeeling-Kalimpong Himalaya.

Table 1. Software used for landslide susceptibility mapping.

Sl. No.	Software	Purpose
1	ArcGIS	Preparation of thematic layers, spatial analysis, raster processing and map generation
2	ArcGIS Pro	Advanced geospatial analysis, cartographic visualization and final map preparation
3	Google Earth Engine	Satellite data processing, NDVI generation and large-scale geospatial analysis
4	Microsoft Excel	Data organization, statistical calculation, AHP computation and result tabulation
5	Microsoft Word	Research-paper drafting, formatting and documentation
6	Google Earth Pro	Visual interpretation and validation support for landslide locations

Table 2. Spatial data layers used in the study.

Sl. No.	Data layer	Source	Purpose
1	DEM	SRTM (USGS EarthExplorer)	Derivation of slope, aspect, curvature, SPI, TWI and relative relief
2	Drainage density	Derived from DEM	Hydrological factor influencing erosion and landslide occurrence
3	Distance to drainage	Derived from DEM	Assessment of drainage influence on slope instability
4	Slope	Derived from DEM	Topographic control on shear stress and slope failure
5	Aspect	Derived from DEM	Slope orientation and related moisture/vegetation conditions
6	Curvature	Derived from DEM	Terrain convergence, divergence and runoff accumulation
7	Relative relief	Derived from DEM	Terrain ruggedness and local elevation variation
8	Stream Power Index	Derived from DEM	Runoff energy and erosion potential
9	Topographic Wetness Index	Derived from DEM	Soil moisture accumulation potential
10	Lineament density	Derived from DEM/structural interpretation	Structural control on rock-mass weakness
11	Distance to lineament	Derived from lineament layer	Influence of geological discontinuities
12	Lithology	Geological Survey of India	Rock type and resistance to weathering
13	Soil map	FAO	Soil texture and stability-related properties
14	Geomorphology	Geological Survey of India	Landform characterization
15	NDVI	Google Earth Engine	Vegetation density and slope-reinforcement assessment
16	Land use/land cover	ESRI Land Cover	Anthropogenic and vegetation-cover influence
17	Rainfall	Indian Meteorological Department	Rainfall-induced landslide triggering
18	Landslide inventory	NASA Global Landslide Catalog	Model support and validation reference

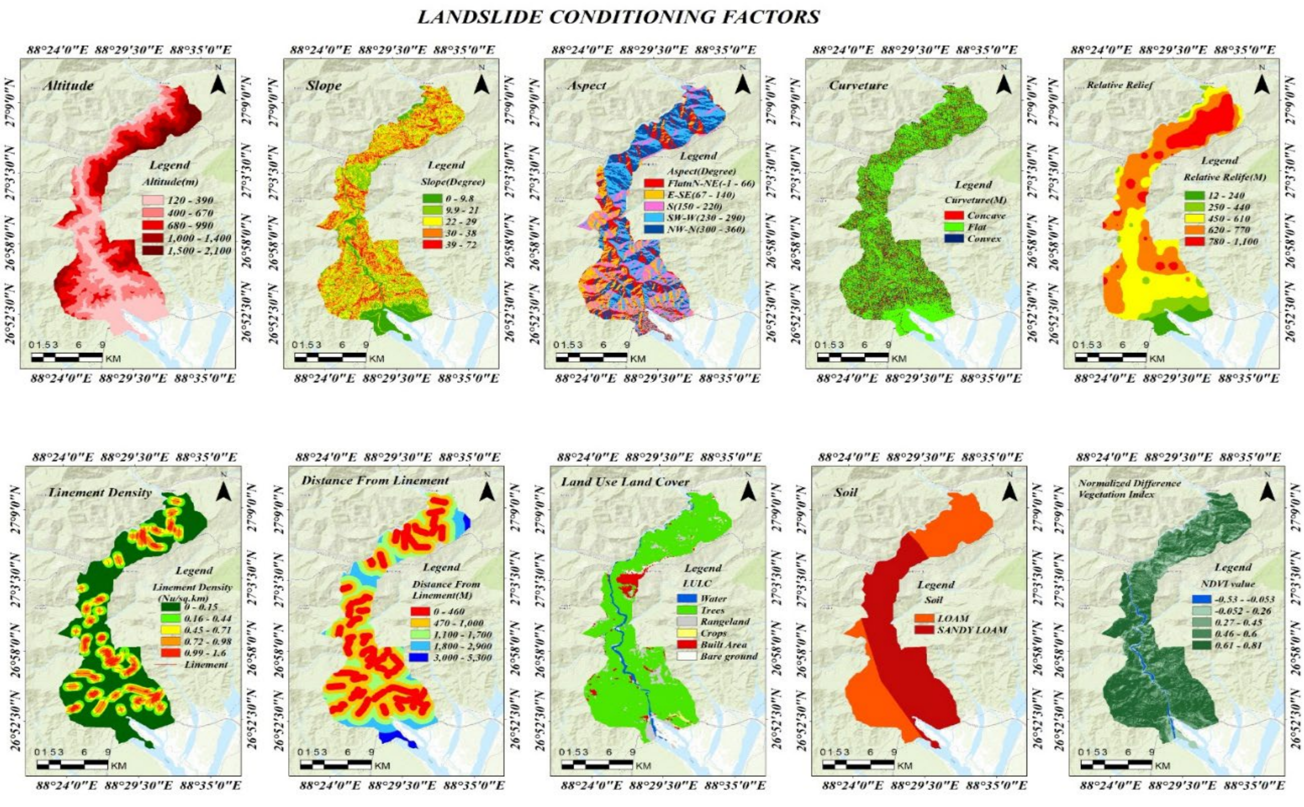

Figure 2. Topographic and hydrological landslide-conditioning layers used in the susceptibility assessment.

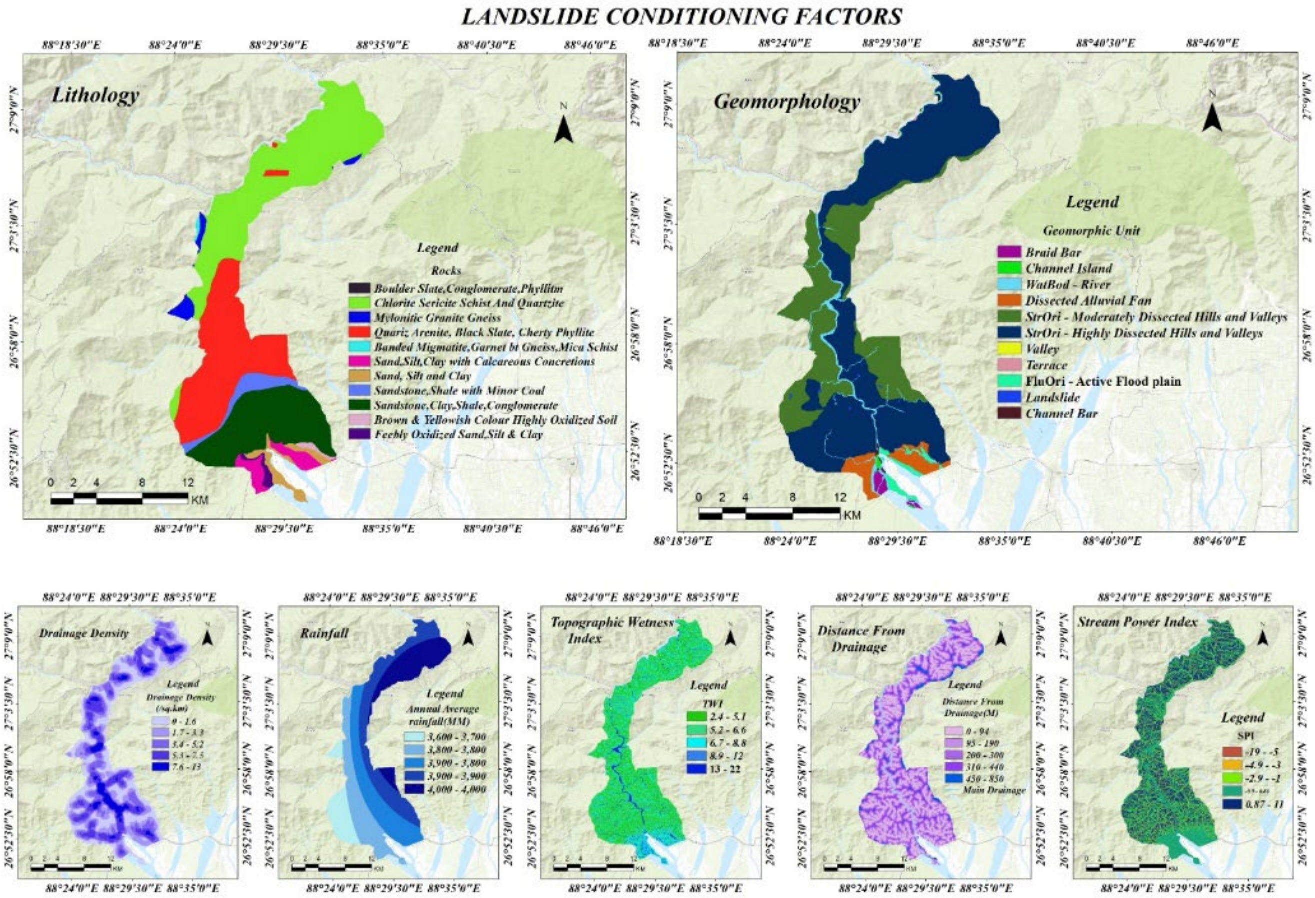

Figure 3. Lithological, geomorphological, land-cover, vegetation and distance-based conditioning layers

2.3 Landslide-conditioning factors

Seventeen landslide-conditioning factors were selected because they represent the principal topographic, structural, hydrological, lithological, climatic, soil, vegetation and land-cover controls on slope instability. The selected factors were altitude, slope, aspect, curvature, relative relief, lineament density, distance from lineament, LULC, soil, NDVI, lithology, geomorphology, drainage density, rainfall, TWI, distance from drainage and SPI (Table 1 and 2) . Each factor was reclassified into susceptibility-related classes based on terrain behavior, expert judgment and evidence from published landslide susceptibility studies (Dai & Lee, 2002; Van Westen et al., 2008).

3. METHODOLOGY

3.1 Analytic Hierarchy Process

The Analytic Hierarchy Process (AHP) was used to assign weights to the conditioning factors. A pairwise comparison matrix was prepared using Saaty's nine-point scale, where relatively more influential factors were assigned higher comparative importance (Table 3 and 5). The pairwise judgments were normalized to generate factor weights (Table 4). The internal consistency of the matrix was evaluated using the Consistency Index and Consistency Ratio. A Consistency Ratio below 0.10 was considered acceptable, in accordance with the AHP standard (Saaty, 1980).

3.2 Weighted overlay and susceptibility classification

The weighted thematic layers were combined in GIS using weighted overlay analysis to calculate the Landslide Susceptibility Index. The general logic of the overlay can be expressed as $LSI = \Sigma(W_i \times R_i)$, where W_i is the normalized weight of the ith conditioning factor and R_i is the reclassified rating of each factor class. The final LSI raster was classified into five susceptibility zones: very low, low, moderate, high and very high. This classification provides a relative spatial interpretation of landslide-prone areas rather than a temporal forecast of landslide occurrence.

3.3 Validation approach

The preliminary validation of the AHP weighting process was based on the consistency test. The calculated Consistency Ratio was 0.092, which is lower than the accepted threshold of 0.10. This confirms that the pairwise comparison was internally consistent. However, consistency validation is not equivalent to field-based predictive validation. Therefore, the susceptibility map should be further tested using independent landslide inventory points, field observations or ROC-AUC analysis in future work.

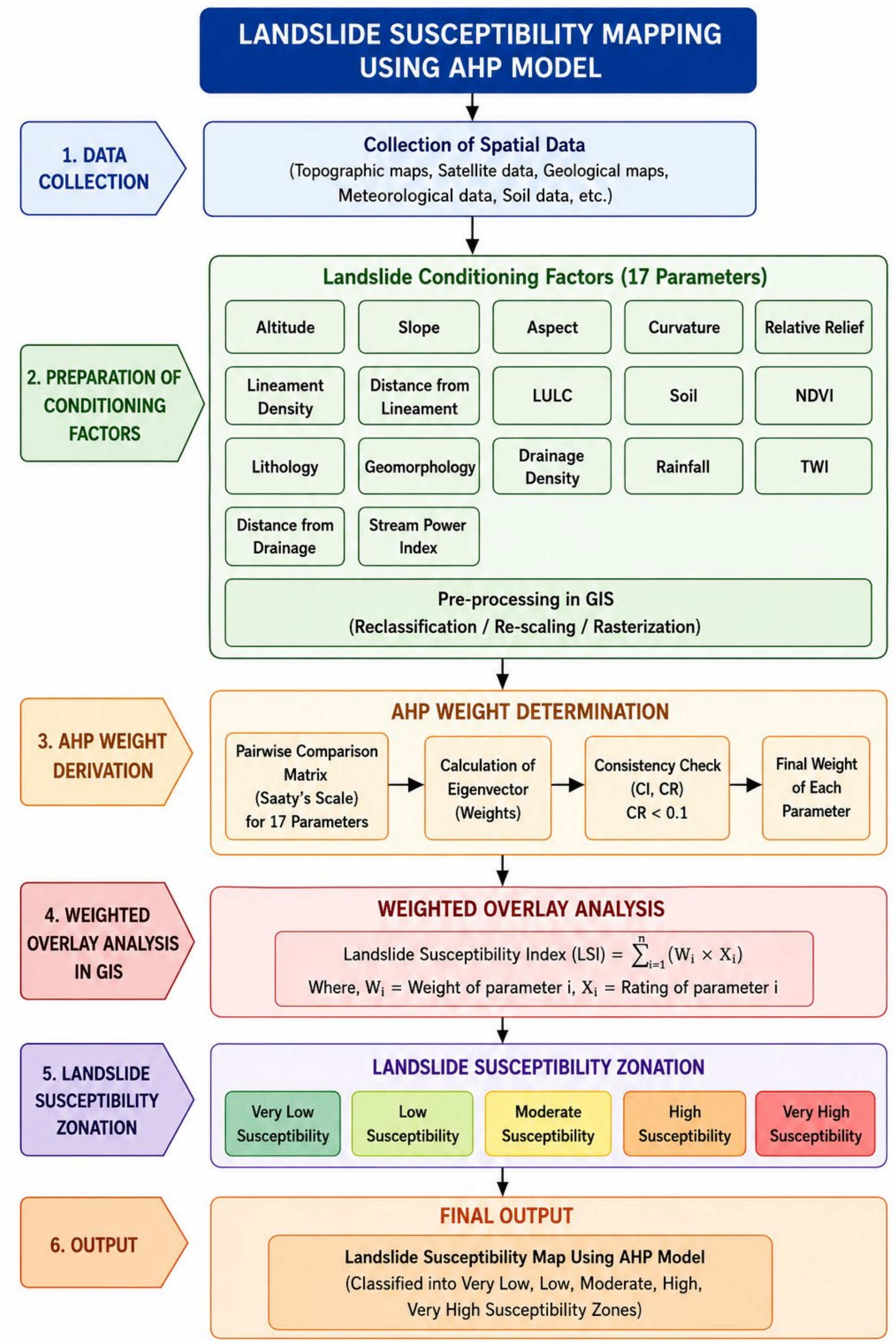

Figure 4. Methodological workflow for AHP-based landslide susceptibility mapping.

Table 3. Pair-Wise Matrix

Name	Lithology	Slope Angle	Drainage	Rainfall	Soil	Geomorphology	Relative Relief	LD	Slope Curvature	LULC	Distance From Drainage	Distance From Lineament	SPI	TWI	NDVI	Slope Aspect	Altitude
	PAIR-WISE MATRIX																
Lithology	1.00	0.50	0.50	0.50	2.00	0.50	2.00	0.50	0.50	0.50	0.50	0.50	0.20	0.50	0.50	0.50	0.20
Slope Angle	2.00	1.00	2.00	2.00	2.00	2.00	2.00	0.50	2.00	2.00	2.00	2.00	2.00	0.50	2.00	0.50	0.20
Drainage	2.00	0.50	1.00	0.50	2.00	0.50	2.00	0.50	2.00	2.00	2.00	2.00	2.00	0.50	2.00	0.50	0.50
Rainfall	2.00	0.50	2.00	1.00	2.00	0.50	2.00	2.00	0.50	3.00	0.50	2.00	2.00	0.50	2.00	0.50	0.50
Soil	0.50	0.50	0.50	0.50	1.00	0.50	0.50	0.50	0.50	2.00	2.00	0.50	0.50	0.50	0.50	0.33	0.20
Geomorphology	2.00	0.50	2.00	2.00	2.00	1.00	2.00	0.50	0.50	2.00	0.50	2.00	0.50	0.50	0.50	0.33	0.50
Relative Relief	0.50	0.50	0.50	0.50	2.00	0.50	1.00	0.50	0.20	2.00	0.50	0.50	2.00	0.50	0.50	0.33	0.33
LD	2.00	2.00	2.00	0.50	2.00	2.00	2.00	1.00	0.50	2.00	0.50	0.50	0.50	0.50	2.00	0.50	0.50
Slope Curvature	2.00	0.50	0.50	2.00	2.00	2.00	5.00	2.00	1.00	2.00	2.00	2.00	2.00	0.50	2.00	0.50	0.50
LULC	2.00	0.50	0.50	0.33	0.50	0.50	0.50	0.50	0.50	1.00	0.50	0.50	0.50	0.50	0.50	0.50	0.33
Distance From Drainage	2.00	0.50	0.50	2.00	0.50	2.00	2.00	2.00	0.50	2.00	1.00	0.50	0.50	0.50	0.50	0.50	0.33
Distance From Lineament	2.00	0.50	0.50	0.50	2.00	0.50	2.00	2.00	0.50	2.00	2.00	1.00	0.50	0.50	0.50	0.50	0.20
SPI	5.00	0.50	0.50	0.50	2.00	2.00	0.50	2.00	0.50	2.00	2.00	2.00	1.00	0.50	0.50	0.50	0.20
TWI	2.00	2.00	2.00	2.00	2.00	2.00	2.00	2.00	2.00	2.00	2.00	2.00	2.00	1.00	0.50	0.50	0.20
NDVI	2.00	0.50	0.50	0.50	2.00	2.00	2.00	0.50	0.50	2.00	2.00	2.00	2.00	2.00	1.00	0.50	0.20
Slope Aspect	2.00	2.00	2.00	2.00	3.00	3.00	3.00	2.00	2.00	2.00	2.00	2.00	2.00	2.00	2.00	1.00	0.50
Altitude	5.00	5.00	2.00	2.00	5.00	2.00	3.00	2.00	2.00	3.00	3.00	5.00	5.00	5.00	5.00	2.00	1.00
Total	**36.00**	**18.00**	**19.50**	**19.33**	**34.00**	**23.50**	**33.50**	**21.00**	**16.20**	**33.50**	**25.00**	**27.00**	**25.20**	**16.50**	**22.50**	**10.00**	**6.40**

Table 4: Normalise Comparison Matrix

	Lithology	Slope Angle	Drainage	Rainfall	Soil	Geomorphology	Relative Relief	Lineament Density	Slope Curvature	LULC	Distance From Drainage	Distance From Lineament	SPI	TWI	NDVI	Slope Aspect	Altitude	Weights (Average)	Lemda (λ)
Lithology	0.03	0.03	0.03	0.03	0.06	0.02	0.06	0.02	0.03	0.01	0.02	0.02	0.01	0.03	0.02	0.05	0.03	0.03	18.69
Slope Angle	0.06	0.06	0.1	0.1	0.06	0.09	0.06	0.02	0.12	0.06	0.08	0.07	0.08	0.03	0.09	0.05	0.03	0.07	19.31
Drainage	0.06	0.03	0.05	0.03	0.06	0.02	0.06	0.02	0.12	0.06	0.08	0.07	0.08	0.03	0.09	0.05	0.08	0.06	19.1
Rainfall	0.06	0.03	0.1	0.05	0.06	0.02	0.06	0.1	0.03	0.09	0.02	0.07	0.08	0.03	0.09	0.05	0.08	0.06	19
Soil	0.01	0.03	0.03	0.03	0.03	0.02	0.01	0.02	0.03	0.06	0.08	0.02	0.02	0.03	0.02	0.03	0.03	0.03	18.87
Geomorphology	0.06	0.03	0.1	0.1	0.06	0.04	0.06	0.02	0.03	0.06	0.02	0.07	0.02	0.03	0.02	0.03	0.08	0.05	18.76
Relative Relief	0.01	0.03	0.03	0.03	0.06	0.02	0.03	0.02	0.01	0.06	0.02	0.02	0.08	0.03	0.02	0.03	0.05	0.03	18.97
Lineament Density	0.06	0.11	0.1	0.03	0.06	0.09	0.06	0.05	0.03	0.06	0.02	0.02	0.02	0.03	0.09	0.05	0.08	0.06	19
Slope Curvature	0.06	0.03	0.03	0.1	0.06	0.09	0.15	0.1	0.06	0.06	0.08	0.07	0.08	0.03	0.09	0.05	0.08	0.07	19.15
LULC	0.06	0.03	0.03	0.02	0.01	0.02	0.01	0.02	0.03	0.03	0.02	0.02	0.02	0.03	0.02	0.05	0.05	0.03	18.7
Distance From Drainage	0.06	0.03	0.03	0.1	0.01	0.09	0.06	0.1	0.03	0.06	0.04	0.02	0.02	0.03	0.02	0.05	0.05	0.05	18.9
Distance From Lineament	0.06	0.03	0.03	0.03	0.06	0.02	0.06	0.1	0.03	0.06	0.08	0.04	0.02	0.03	0.02	0.05	0.03	0.04	18.77
SPI	0.14	0.03	0.03	0.03	0.06	0.09	0.01	0.1	0.03	0.06	0.08	0.07	0.04	0.03	0.02	0.05	0.03	0.05	18.9
TWI	0.06	0.11	0.1	0.1	0.06	0.09	0.06	0.1	0.12	0.06	0.08	0.07	0.08	0.06	0.02	0.05	0.03	0.07	19.35
NDVI	0.06	0.03	0.03	0.03	0.06	0.09	0.06	0.02	0.03	0.06	0.08	0.07	0.08	0.12	0.04	0.05	0.03	0.05	19.28
Slope Aspect	0.06	0.11	0.1	0.1	0.09	0.13	0.09	0.1	0.12	0.06	0.08	0.07	0.08	0.12	0.09	0.1	0.08	0.09	19.24
Altitude	0.14	0.28	0.1	0.1	0.15	0.09	0.09	0.1	0.12	0.09	0.12	0.19	0.2	0.3	0.22	0.2	0.16	0.16	19.37
Total																			**19.37**

CI: 0.148377; RCI: 1.61; CR (CI/RCI): 0.09216

Table 5: Random Consistency Index (Saaty, 1980)

n	1	2	3	4	5	6	7	8	9	10	11	12	13	14	15	16	17
RCI	0	0	0.6	1	1.1	1.2	1.3	1.4	1.5	1.49	1.51	1.48	1.56	1.57	1.59	1.6	1.61

4. RESULTS

4.1 Terrain and environmental controls

Elevation in the study area ranges from approximately 120 m to 2,100 m, with higher and more rugged terrain occurring toward the northern and north-eastern sectors. Higher elevation zones generally coincide with steeper slope gradients, stronger weathering, higher erosion rates and greater geomorphic activity. Slope values range from nearly flat terrain to approximately 72°, indicating strong topographic contrast. Steep slopes are more susceptible because gravitational shear stress increases and runoff become more erosive.

Aspect influences solar exposure, soil moisture, vegetation growth and weathering. Curvature controls the convergence and divergence of surface water: concave slopes favor water accumulation and saturation, whereas convex slopes encourage runoff dispersion. Relative relief varies from about 12 m to 1,100 m, showing that terrain ruggedness is an important control. Areas with high relative relief are generally associated with deeply dissected hill slopes and active erosion.

Lineament density and distance from lineament represent structural controls. Areas close to faults, fractures, joints or shear zones are generally more susceptible because discontinuities weaken the rock mass and promote water infiltration. Lithology further controls slope resistance. Weak, fractured and weathered units such as phyllite, shale, sandstone and unconsolidated deposits are more prone to failure than more competent rock units such as quartzite and gneiss.

Drainage density, distance from drainage, TWI and SPI indicate the role of water and fluvial erosion. High drainage density and high SPI values are associated with active runoff, channel incision and slope undercutting. High TWI zones occur in valley bottoms and flow convergence areas, where prolonged moisture accumulation may increase pore-water pressure and reduce soil cohesion. Rainfall, which ranges broadly between about 3,600 and 4,000 mm annually, is a major triggering factor because intense and prolonged rainfall increases saturation and weakens slope materials.

LULC and NDVI represent the combined effects of vegetation cover and anthropogenic disturbance. Dense vegetation can improve soil reinforcement through root networks and reduce runoff, whereas bare land, built-up areas, road cuts and disturbed slopes tend to have higher susceptibility. Soil type influences infiltration, cohesion and shear strength; loam and sandy loam soils may behave differently under prolonged rainfall depending on texture, permeability and degree of saturation.

4.2 AHP consistency and model reliability

The AHP model produced a Consistency Ratio of 0.092. Because this value is below 0.10, the weighting scheme was considered acceptable for susceptibility modelling. The result indicates that the pairwise judgments were mathematically coherent and suitable for weighted overlay analysis. Nevertheless, the model should be interpreted as a regional-scale susceptibility tool and not as a deterministic landslide prediction model.

4.3 Landslide susceptibility zones

The final landslide susceptibility map classified the Teesta River Basin into five zones: very low, low, moderate, high and very high susceptibility. The spatial pattern is not uniform. A clear north-to-south gradient is visible, with the northern and central mountainous blocks showing greater susceptibility than the southern foothill and relatively low-gradient areas. Kalimpong and Kalimpong-I are dominated by high and very high susceptibility zones, especially along steep hill slopes and river valleys. Kurseong is mainly represented by low to moderate susceptibility with isolated high-susceptibility pockets, whereas Matigara has comparatively lower susceptibility.

The moderate class occupies the largest area (69.85 km^2; 28.53%), followed closely by the high class (68.74 km^2; 28.07%). Together, moderate and high susceptibility zones account for more than half of the study area, indicating widespread terrain instability potential. The very high class covers 37.87 km^2 (15.46%), representing priority zones for detailed field investigation, slope stabilization and development control.

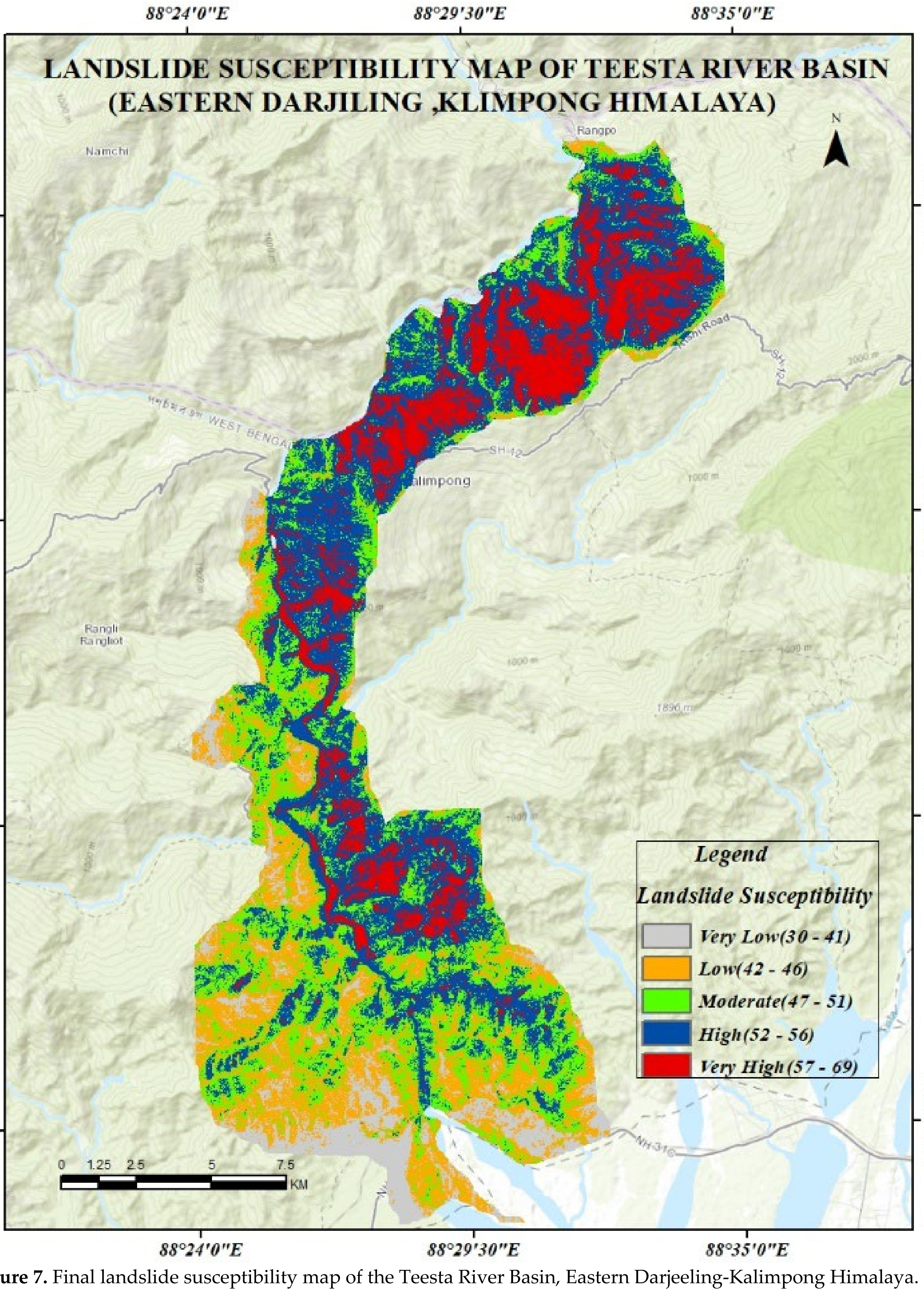

Figure 7. Final landslide susceptibility map of the Teesta River Basin, Eastern Darjeeling-Kalimpong Himalaya.

Table 3. Area distribution of landslide susceptibility classes.

Susceptibility class	Area (km²)	Share of study area (%)
Very low	19.48	7.95
Low	48.94	19.99
Moderate	69.85	28.52
High	68.74	28.07
Very high	37.87	15.46
Total	**244.88**	**100.00**

6. DISCUSSION

The susceptibility pattern confirms that landslide occurrence in the Teesta Himalayan landscape is controlled by a combination of terrain steepness, relief, drainage incision, lithological weakness, rainfall and vegetation disturbance. The concentration of high and very high susceptibility zones in the northern and central mountainous sectors is consistent with the geomorphic setting of the basin, where steep slopes, rugged terrain and high fluvial incision dominate. This spatial pattern is comparable with earlier landslide susceptibility studies in the Darjeeling-Sikkim Himalaya, which also reported strong control of slope, lithology, rainfall, drainage and land-cover variables (Kundu & Ghosh, 2025; Mandal et al., 2023; Poddar & Roy, 2024).

The AHP-GIS framework is useful for the present study because it can integrate multiple heterogeneous factors in a transparent and reproducible way. It is especially appropriate where detailed geotechnical information and continuous field-based landslide inventories are limited. However, AHP also has a known limitation: the weights depend partly on expert judgment. A mathematically acceptable consistency ratio reduces internal contradiction in the weights but does not automatically prove predictive accuracy. This is why independent validation using landslide inventory points, field checks or ROC-AUC analysis is necessary before using the map for high-stakes engineering decisions.

From a planning perspective, areas under high and very high susceptibility should be treated as priority zones for detailed field assessment, slope drainage improvement, road-cut stabilization, controlled excavation, retaining structures where technically justified, and regulated construction. Moderate susceptibility zones also require caution because triggering events such as intense rainfall, poor drainage, slope cutting or vegetation removal can shift them toward higher instability. Low and very low zones should not be interpreted as completely safe; they only represent lower relative susceptibility under the selected model and available datasets.

The study provides a regional-scale landslide susceptibility map that can support disaster risk reduction, land-use planning, road and infrastructure alignment, watershed management and environmental planning. The map can help administrators and planners prioritize areas for detailed geotechnical investigation, rainfall monitoring, drainage improvement and community-level preparedness. It is also useful as a baseline layer for future hazard, vulnerability and risk studies in the Teesta River Basin.

- The study does not include detailed subsurface information such as groundwater levels, soil depth, rock discontinuity measurements, shear-strength parameters or geotechnical borehole data.
- Field verification was limited; therefore, susceptibility classes should be checked through ground survey before site-specific engineering decisions are made.
- AHP uses expert judgment, so factor weights can vary depending on evaluator experience, data quality and regional knowledge.
- The model represents relative spatial susceptibility and does not predict the timing of landslide occurrence.
- Future improvement should include high-resolution DEMs, updated landslide inventory data, real-time rainfall information and statistical or machine-learning validation.

5. CONCLUSION

This study developed a GIS and AHP-based landslide susceptibility map for the Teesta River Basin in the Eastern Darjeeling-Kalimpong Himalaya. Seventeen conditioning factors representing terrain, lithology, geomorphology, drainage, rainfall, vegetation, soil and land-cover controls were integrated through weighted overlay analysis. The AHP weighting process produced a Consistency Ratio of 0.092, indicating acceptable internal consistency.

The final map divided the basin into very low, low, moderate, high and very high susceptibility zones. Moderate and high susceptibility classes occupied the largest areas, while very high susceptibility zones were concentrated mainly in the northern and central mountainous sectors, especially around Kalimpong and Kalimpong-I. These areas are characterized by steep slopes, high relative relief, drainage incision, weak lithological units, high rainfall and structural discontinuities.

The generated map provides a practical decision-support tool for slope hazard management, land-use regulation, infrastructure planning, watershed management and disaster risk reduction. For operational use, the map should be supplemented with field validation, updated landslide inventory data, detailed geotechnical information and rainfall-trigger analysis. Overall, the study confirms that the integration of GIS, Remote Sensing and AHP is an effective regional-scale approach for landslide susceptibility assessment in fragile Himalayan terrain.

Conflicts of Interest: The authors declare no conflicts of interest.

Funding: This research received no external funding.

Acknowledgments: NA

Author Contributions: The authors confirm equal responsibility for the following: study conception and design, data collection, analysis and interpretation of results, and preparation of the manuscript.

AI Disclosure: The authors declare that artificial intelligence (AI) tools were used solely to assist in language refinement, organization, and editing of the manuscript. AI was not used to generate original research data, conduct analyses, or draw scientific conclusions. All technical content, interpretations, and final decisions were developed and verified by the authors, who take full responsibility for the accuracy, integrity, and originality of the work.

REFERENCES

Ayalew, L., & Yamagishi, H. (2005). The application of GIS-based logistic regression for landslide susceptibility mapping in the Kakuda-Yahiko Mountains, central Japan. Geomorphology, 65(1-2), 15-31. https://doi.org/10.1016/j.geomorph.2004.06.010

Bachri, S., Shrestha, R. P., Utaya, S., Sumarmi, Prastiwi, M., Putri, N., & Hidiyah, T. (2025). Landslide susceptibility assessment through bivariate models (weight of evidence and frequency ratio) in Pesanggaran, East Java, Indonesia. Geoenvironmental Disasters, 12(1), Article 41.

Bonham-Carter, G. F. (1994). Geographic information systems for geoscientists: Modelling with GIS. Pergamon Press.

Dai, F. C., & Lee, C. F. (2002). Landslide characteristics and slope instability modeling using GIS, LiDAR, and probabilistic methods. Geomorphology, 42(3-4), 213-228. https://doi.org/10.1016/S0169-555X(01)00087-3

Fell, R., Corominas, J., Bonnard, C., Cascini, L., Leroi, E., & Savage, W. Z. (2008). Guidelines for landslide susceptibility, hazard and risk zoning for land-use planning. Engineering Geology, 102(3-4), 85-98. https://doi.org/10.1016/j.enggeo.2008.03.022

Guzzetti, F., Mondini, A. C., Cardinali, M., Fiorucci, F., Santangelo, M., & Chang, K. T. (2012). Landslide inventory maps: New tools for an old problem. Earth-Science Reviews, 112(1-2), 42-66. https://doi.org/10.1016/j.earscirev.2012.02.001

Guzzetti, F., Reichenbach, P., Cardinali, M., Galli, M., & Ardizzone, F. (2005). Probabilistic landslide hazard assessment at the basin scale. Geomorphology, 72(1-4), 272-299. https://doi.org/10.1016/j.geomorph.2005.06.002

Kayastha, P., Dhital, M. R., & De Smedt, F. (2013). Application of the analytical hierarchy process (AHP) for landslide susceptibility mapping: A case study from the Tinau watershed, west Nepal. International Journal of Geomatics and Geosciences, 3(3), 595-610.

Kundu, S., & Ghosh, S. (2025). GIS-integrated landslide susceptibility mapping in the Teesta River Basin of the Darjeeling-Sikkim Himalaya: A comparative analysis of frequency ratio, logistic regression models, and analytical hierarchy process. In Progress in multicriteria decision making models: A new paradigm to monitor hazards (pp. 131-169). Springer Nature Switzerland.

Lee, S., & Pradhan, B. (2007). Landslide hazard mapping at Selangor, Malaysia using frequency ratio and logistic regression models. Landslides, 4(1), 33-41. https://doi.org/10.1007/s10346-006-0047-y

Mandal, B., Biswas, B., & Mandal, S. (2026). Application of bivariate statistical models to explore landslide susceptibility and risk in the Lish River basin of Darjeeling Himalaya. Environment, Development and Sustainability, 28(4), 8225-8274.

Mandal, B., Mondal, S., & Mandal, S. (2023). GIS-based landslide susceptibility zonation (LSZ) mapping of Darjeeling Himalaya, India using weights of evidence (WoE) model. Arabian Journal of Geosciences, 16(7), Article 421.

Pitchaimani, V. S., Joe, R. J., Stuvar, S. R., Liberthin, M., Promilton, A. A. A., & Abishek, S. R. (2026). Landslide susceptibility and vulnerability assessment using GIS-AHP in the highland of Wayanad, Western Ghats, India. Discover Hazards, 2(1), Article 5.

Poddar, I., & Roy, R. (2024). Application of GIS-based data-driven bivariate statistical models for landslide prediction: A case study of highly affected landslide prone areas of Teesta River basin. Quaternary Science Advances, 13, Article 100150.

Pradhan, B., & Lee, S. (2010). Regional landslide susceptibility analysis using GIS, remote sensing, and statistical models in the mountainous regions. Environmental Earth Sciences, 61(2), 215-230.

Reichenbach, P., Rossi, M., Malamud, B. D., Mihir, M., & Guzzetti, F. (2018). A review of statistically based landslide susceptibility models. Earth-Science Reviews, 180, 60-91. https://doi.org/10.1016/j.earscirev.2018.03.001

Saaty, T. L. (1980). The analytic hierarchy process. McGraw-Hill.

Sarkar, S., Kanungo, D. P., Patra, A. K., & Kumar, P. (2013). GIS-based landslide susceptibility mapping in the Indian Himalaya. Natural Hazards, 68(2), 839-861.

Van Westen, C. J., Castellanos, E., & Kuriakose, S. L. (2008). Spatial data for landslide susceptibility, hazard, and vulnerability assessment: An overview. Engineering Geology, 102(3-4), 112-131. https://doi.org/10.1016/j.enggeo.2008.03.010